Variation in wind and crown fire behaviour in a northern jack pine – black spruce forest[1]

S.W. Taylor, B.M. Wotton, M.E. Alexander, and G.N. Dalrymple

Abstract: Fire spread and flame temperature were examined in a series of nine experimental crown fires conducted in the Northwest Territories, Canada. Average rates of spread were 17.8–66.8 m·min^{-1} (0.3–1.1 m·s^{-1}) over burning periods from about 1.5–10 min across 75 m × 75 m to 150 m × 150 m plots. Detailed maps of fire front progression revealed areas with higher rates of spread in the order of tens of metres in horizontal dimension and tens of seconds in duration in several of the fires, which is consistent with the influence of coherent wind gusts. Comparison of open and in-stand wind speed before and after burning suggests that defoliation in the canopy layer during burning would result in the flaming zone having greater exposure to the ambient wind. Estimates of flame front residence from video observations at the surface averaged 34 s; estimates from temperature measurements decreased significantly with height from 74 s at the surface to 31 s below the canopy.

Résumé : La propagation du feu et la température des flammes ont été étudiées lors d'une série de neuf feux de cime déclenchés à des fins expérimentales dans les Territoires du Nord-Ouest au Canada. Le taux moyen de propagation variait de 17,8 à 66,8 m·min^{-1} (0,3 à 1,1 m·s^{-1}) au cours de périodes de brflage d'environ 1,5 à 10 min d'un côté à l'autre de places échantillons carrées de 75 m × 75 m à 150 m × 150 m. Des cartes détaillées de la progression du front du feu ont mis en évidence des zones oj le taux de propagation était plus élevé de l'ordre de dizaines de mètres horizontalement pendant des dizaines de secondes dans le cas de plusieurs des feux; ce qui concorde avec l'influence de rafales de vent correspondantes. La comparaison de la vitesse du vent à l'extérieur et à l'intérieur du peuplement avant et après le brflage indique que la défoliation dans la canopée causée par le feu faisait en sorte que la zone de flammes était davantage exposée au vent ambiant. Le temps que prenait le front de flammes pour franchir un point donné, estimé à l'aide d'observations vidéo à la surface, était en moyenne de 34 s; les estimations obtenues à partir des mesures de température diminuaient fortement avec la hauteur, soit de 74 s à la surface à 31 s sous la canopée.

[Traduit par la Rédaction]

Introduction

One of the main themes of forest fire research has been to relate fire behaviour to the attendant environmental conditions. In previous experiments in Canada, referred to by Stocks et al. (2004*a*, 2004*b*), the average fire spread rate across plots in the order of 50–100 m in length and average wind speed over a period of minutes were measured. The rate-of-spread equations in the Canadian Forest Fire Behavior Prediction (FBP) System (Forestry Canada Fire Danger Group 1992) are based largely on empirical correlations among average fire spread rates and average 10-m open wind speed, fine fuel moisture content (expressed through the Initial Spread Index (ISI) component of the Canadian Forest Fire Weather Index (FWI) System (Van Wagner 1987)), and a build-up effect representing the effect of fuel consumption. The effects of fire-induced circulation (as a result of connective buoyancy) on fire spread are not explicitly accounted for in the Canadian FBP System or other empirical models (e.g., Rothermel 1972; Sneeuwagjt and Peet 1985; Forestry Canada Fire Danger Group 1992). The effect of fire-induced circulation may be implicitly accounted for if observations of large, free-burning wildfires are included in empirical models, especially for severe burning conditions, as they are in most of the rate-of-spread equations contained in the Canadian FBP System. Coupled empirical–atmospheric models (e.g., Clark et al. 1996) and physically based models (e.g., Linn et al. 2002) account for three-dimensional, fire–atmospheric circulation but have not as yet been tested against a wide range of empirical observations, in part because they are computationally demanding. It is likely that empirical models will continue to have a place in fire management for some time because of their relative simplicity.

The Canadian FBP System and other empirical fire spread models are usually applied assuming a constant wind speed and so predict a quasi-steady state spread rate — mean forward fire spread rate is predicted by mean fuel load and other environmental variables (Cheney and Gould 1995). While me-

Received 8 March 2004. Accepted 29 June 2004. Published on the NRC Research Press Web site at http://cjfr.nrc.ca on 19 August 2004.

S.W. Taylor[2] and G.N. Dalrymple. Canadian Forest Service, Pacific Forestry Centre, 506 W. Burnside Rd., Victoria, BC, V8Z 1M5, Canada.
B.M. Wotton. Canadian Forest Service, Great Lakes Forestry Centre, 1219 Queen St. East, Sault Ste. Marie, ON P6A 2E5, Canada.
M.E. Alexander. Canadian Forest Service, Northern Forestry Centre, 5320–122 St., Edmonton, AB, T6H 3S5, Canada.

[1]This article is one of a selection of papers published in this Special Issue on The International Crown Fire Modelling Experiment (ICFME) in Canada's Northwest Territories: Advancing the Science of Fire Behaviour.
[2]Corresponding author (e-mail: staylor@nrcan.gc.ca).

 doi: 10.1139/X04-116

teorologists commonly describe the surface wind using average values over periods of 10–20 min, the winds acting on a free-burning fire are rarely constant. The wind speed at a fixed point in the atmosphere varies randomly on different time scales ranging from years down to minutes or seconds (Boettcher et al. 2003). The forest canopy in which crown fires occur (which is in the order of about 5–20 m tall in the boreal forest) is near the bottom of a turbulent atmospheric boundary layer approximately 500–1000 m deep (Kaimal and Finnigan 1994). Wind in the atmospheric boundary layer is turbulent and unstable as a result of sheer stresses as air flows over objects on the surface, thermal gradients, and the earth's rotation. A rotating eddy of air in the prevailing wind field is experienced as a gust at the surface. Gusts can be of any size from a diameter of the order of millimeters to the depth of the boundary layer. Furthermore, the drag exerted by the forest canopy causes turbulence and strongly reduces wind speed within and below the canopy (Finnigan and Brunet 1995). Turbulence beneath the canopy is dominated by large, coherent eddies at the scale of the canopy height (Finnigan 2000). The mean wind-speed profile in forests is often approximated by a logarithmic curve beginning above the canopy with a strong inflection point near the top of the canopy, which becomes even stronger during gusts (Raupach et al. 1996). The degree of attenuation and shape of the curve below the canopy may depend on stand density and the amount of understory vegetation (Reifsnyder 1955).

The effects of variation in wind speed on forest fire spread dynamics are generally not well known. This is in part because it is not simple to measure the rate of spread of high-intensity fires at fine spatial and temporal scales, nor is it simple to measure the wind at the edge of a rapidly moving fire front in large, free-burning forest fires. For example, Anderson et al. (1982) found greater variation in fire spread than in wind speed in grass fires in Australia. Cheney (1981), also studying grass fires in Australia, found that spread rates increased in a stepwise fashion because of gusts and changes in wind direction that increased the width of the fire front. Albini (1982*a*) postulated that fire spread rate increases instantaneously in response to increasing wind speed because of the typical characteristic time and space domains of wildland fires. The time elapsed between arrival of fire at a given point and the end of flaming combustion is in the range of 0.5–2 min. The thermal relaxation time for fine fuels that determine spread rate is about 1 s. The transit time of hot gasses from surface to flame tip about 1 s, and the transit time for winds blowing at 1–10 $m \cdot s^{-1}$ across the flaming zone is less than 1 s. He suggested that the response is nonlinear because the instantaneous rate of fire spread is proportional to U^3/I (where U is wind speed and I is fire intensity), but fire intensity cannot change instantaneously, since it is proportional to the volume of the burning zone. Albini (1982*a*) further suggested that a fire should behave like a second-order damped system in response to a sudden change in wind speed. The fire should race ahead as intensity lags then slow as fire intensity rises and buoyancy increases. Because of this damping effect, the variation in fire spread amplitude is not solely dependent on the variation in the wind-speed amplitude but varies with the frequency of the wind-speed cycle and differs between fuel types depending on the flame front residence time. Using numerical simulation, Morvan et al. (2002) also predicted that the spread rate and intensity in shrub fires will fluctuate with a constant wind speed because of thermal instability. Beer (1991) suggested that wind gusts affect fire spread rate through flame radiation (as horizontal wind speed increases and tips the flame over) as well as by advective preheating because of downdraft winds associated with gusts. Albini (1982*b*) predicted that the variability in fire spread rate decreases as mean wind speed increases but that the absolute variation increases and that the short-term variation will be large, with the standard deviation exceeding the mean. Applying dimensional analysis to a set of laboratory and field data, Nelson and Adkins (1988) found that fire spread rate r ($m \cdot s^{-1}$) was related to fuel consumption w_a ($kg \cdot m^{-2}$), wind speed u_a ($m \cdot s^{-1}$), and flame front residence time t_r (s).

$$[1] \qquad r = \frac{0.39\, w_a^{0.25}\, u_a^{1.51}}{t_r}$$

If fire spread varies with wind speed to the 1.51 power or greater and fire spread responds instantaneously to short-term variation in wind speed, then higher spread rates should be observed with more variable wind speeds than would be predicted by the mean wind speed.

Living and nonliving elements in or adjacent to a fire are exposed to the instantaneous fire intensity as the fire approaches or passes, not the mean intensity. An understanding and ability to predict variation in fire spread and intensity is important to predict the probability of crowning, fire growth, and ecological effects such as crown scorch and tree mortality. de Groot et al. (2004) found significant spatial variation in viable jack pine (*Pinus banksiana* Lamb.) seed rain following crown fire over distances in the order of tens of metres, which is likely due to spatial variation in fire intensity and the heating of cones in the crown. Variation in fire intensity may also have important fire management implications. Crosby and Chandler (2004) note that variations in spread rate can influence the probability of fire-line breaching. Underestimation of the potential for rapid increases in fire spread due to variations in wind direction (usually associated with gusts) is also thought to be a major factor in fire-line fatalities in Australia (Cheney et al. 2001).

This study was carried out to assess temporal and spatial variation in fire spread rate in relation to wind speed and to characterize flame front residence time during the International Crown Fire Modelling Experiment (ICFME) fires described by Stocks et al. (2004*b*). A better understanding of the variation in wind and fire spread may suggest the further developments and applications of empirical and physically based fire spread models.

Materials and methods

Study site

The fires were conducted in 1931-origin jack pine stands with a black spruce (*Picea mariana* (Mill.) BSP) understory near Fort Providence, Northwest Territories, Canada (61.6°N, 117.2°W). Ten main plots ranging in size from 75 m × 75 m to 150 m × 150 m were burned in weather conditions conducive to crown fire in June and July over four summers (1997–2000). The site characteristics, plot layout,

Table 1. Number of wind, thermocouple, and video observation points by plot and year.

	Plot								
Parameter	1	3	4	5	6	7	8	9	A
Year burned	2000	2000	1999	1997	1997	1998	1998	1999	1997
Wind towers	4	2	4	4	6	3	3	3	2
Surface thermocouples	42	42	31	24	34	32	39	22	15
Thermocouple tower									
9.0 m	3	3	3	3	3	3	3	3	3
3.0 m	–	–	–	2	2	2	2	–	2
Video cameras	3	3	–	–	–	–	1	1	–

stand, fuel, burning conditions, and operational methods are described in detail by Alexander et al. (2004) and Stocks et al. (2004*b*).

Ignition technique

The ICFME experimental plots were ignited on the upwind plot edge, such that the ignition line was perpendicular to the wind direction (Stocks et al. 2004*b*). The ignition was carried out with a truck-mounted Terra-Torch® (Fire Spec Systems, Carmel, California). This device projects a stream of flaming, gelled gasoline up to 20 m. A continuous band of flaming fuel mixture approximately 1 m wide was sprayed on the forest floor surface along the plot edge not more than 2 m into the plot, igniting the surface forest fuels almost immediately. The gelled fuel has a flaming residence time of less than 1 min.

Wind measures

Measurement of wind speed around the fires

Wind speed and direction were measured at 10.0, 5.0, and 2.0 m at a central, open control tower during the course of each year's field sampling, which was located approximately 100–700 m from the plots. In addition, anemometers and wind vanes affixed to 10-m, guyed, metal towers or masts were placed around each plot prior to burning to characterize the wind field during the period of active fire spread. The number and position of the wind towers relative to the burned plot varied over the course of the experiment because of logistical constraints; the number of towers is given in Table 1. There was typically at least one anemometer tower on the ignition side and one on the exit side of the fire. Where there were three or more towers, two towers were located on the two sides parallel to the wind direction. Three anemometers and wind vanes were deployed on each tower at heights of 10.0, 5.0, and 2.0 m above the ground surface. Three different models of instruments were used because of availability constraints. However, the same model of instrument was used at each height between towers: at 10 m, a Weather Measure Corp. 2032 anemometer and 2005 vane; at 5, m an R.M. Young model 05103 wind monitor; at 2, m an R.M. Young 12005 anemometer and vane. In 1997, wind speed and direction were sampled every 5 s at the control and plot-edge towers, and 1-min averages of these quantities were recorded on Campbell Scientific CR-10 dataloggers (Campbell Scientific Canada, Edmonton, Alberta). During 1998–2000, wind speed and direction was sampled and recorded at 5-s intervals at the control and plot-edge towers before, during, and after each fire.

The variance of the 5-s control tower wind speeds was examined using SAS autocorrelation (PROC ARIMA) and spectral analysis (PROC SPECTRA) procedures (SAS Institute Inc. 1993) to determine the stability of wind speeds and periodicity of gusts and lulls around the burning periods.

Comparison of in-stand wind speed before and after burning

Multilevel wind towers were placed in the centre of plot 1 and 3 for several days before and after the plots were burned in 2000. An identical multilevel tower was also erected between plots 1 and 3 (25 m north of the north edge of plot 3 and along the central north–south axis of the plot; see Fig. 1 in Stocks et al. 2004*b*) as well as at the primary control tower location for comparison purposes. Wind-speed averages were measured over 15-min intervals at each of these tower locations at heights of 2.0, 5.0, and 10.0 m. To examine reduction in wind speed within the stand, we compared winds measured inside the plot with winds measured at the two open sites. To avoid large differences when winds were light, we used 15-min averages for comparison from 0900 to 2100 during the day and only if the in-stand wind speed was above 1.0 $km \cdot h^{-1}$.

In-fire video recording

Fire progression within the stands was recorded on videotape in seven experimental fires. A consumer-grade, handheld video camera was placed in an insulated steel box with a viewing port cut out for the lens. The viewing port was covered with an infrared filter, then with a high-temperature, clear glass plate to protect the camera from the heat as the fire passed over (Kautz 1997). Prior to ignition, the camera boxes were placed within the plot to be burned such that a thermologger and thermocouple tower (described later in this section) were in the field of view. The cameras were turned on approximately 30 min before ignition to record the progress of the fire through the field of view. Eight video observations were made in the primary plots (Table 1) and seven observations were in plots B, I-2, and Treated–Untreated, described by Alexander et al. (2004), which had the same fuel conditions and were burned under similar weather conditions.

Fire spread mapping

Fire spread measurements

The surface fire spread pattern and rate of advance were characterized using a grid-sampling scheme. Fire-arrival times

and temperatures were recorded at points on a 15 m × 30 m grid in each plot. However, the number of fire-arrival time and time–temperature samples that were obtained varied between fires because of plot size, logistical constraints, and equipment failure (Table 1).

Thermocouples and dataloggers were installed at the grid points before the fire. Two different purpose-built thermocouple–datalogger systems were used. The Forest Technology Systems (FTS) Ltd. thermologgers (Forest Technology Systems Ltd., Victoria, B.C.) record temperatures on three channels (A, B, C) when channel A exceeds 70 °C at fixed 10-s, 1-min, and 1-min sampling frequencies (0.1, 0.017, 0.017 Hz) on channels A, B, and C, respectively, using type K chromel–alumel, inconel overbraided, ceramic-fiber-insulated, 20 gauge (approximately 1.5 mm diameter) thermocouples with a range of 0–1200 °C. Thermocouple A is sampled at 1-s intervals until the tripping threshold is reached, and so the fire-arrival times are accurate to 1 s. A second type of programmable instrument, forest fire temperature recorders, with similar thermocouples (except the tip was approximately 0.5 mm and functioned over the range 0–1500 °C), was configured to record temperatures at 1-s intervals when one of the thermocouples exceeded 100 °C. The environmentally sealed datalogger portion of both types of instrument was buried in the soil at predetermined sample grid points to shield them from heat during the fire. The tripping thermocouple was fixed at 3 cm above the surface of the forest floor, and the other thermocouples were fixed in the forest floor organic layer, 3 cm below the surface.

Data analysis

Fire-arrival times were determined as the time when the temperature at 3 cm above the forest floor exceeded 100 °C. Surfaces were fitted from the fire-arrival times and the corresponding *x*, *y* coordinates of the sample points using ordinary kriging techniques in Environmental Systems Research Institute (ESRI™, Redlands, California) Geostatistical Analyst (Johnston et al. 2001). Cross validation was carried out to provide an estimate of goodness of fit of the surfaces. In this method, each data point is removed from the data set in turn, the model is refitted, and the deviation of the removed point from the new surface is determined. These measures of deviation are used to estimate the goodness of fit statistics. Isochrons were plotted on the fire-arrival time surfaces at 10-s intervals, and the slope of the surface was determined in ESRI™ Geospatial Analyst. A fire rate of spread (ROS) surface was calculated from the slope of the fire-arrival time surface using the following equation:

$$[2] \qquad \mathrm{ROS} = \tan(90 - \mathrm{slope})$$

Rates of spread were also calculated using the triangulation technique described by Simard et al. (1982, 1984); however, the surface-fitting technique provided a better visualization of fire dynamics. The triangulation method would be more suitable if only a few data points were available.

The location of the point of maximum rate of spread over the course of each fire was determined by first gridding the fire-arrival time and rate of spread surfaces into 1-m cells in ESRI™ Arc 8.0. The fire-arrival times and rate of spread values were then merged on the *x*, *y* coordinates, and the position of the maximum rate of spread at 1-s intervals and the average maximum rate of spread at 5-s intervals were found using a computer program written in the SAS language.

Flame temperature and flame front residence time

Temperature measurements

Thermocouples attached to vertical steel towers were installed in each plot before burning to characterize the vertical flame temperature profile within and below the tree canopy. The average canopy height and height to live crown base was 12.2 and 6.6 m, respectively. Detailed stand characteristics for each plot are given by Alexander et al. (2004). Three 9.0-m tall towers were placed in each of the primary plots 1–8. On each of the towers, seven thermocouples were set at heights of 0.5, 1.0, 2.0, 3.0, 5.0, 7.0, and 8.5 m. The uppermost thermocouple was generally in the bottom of the tree canopy. The thermocouples were Type K chromel–alumel made of 0.005 in. (1 in. = 2.54 cm) diameter wire (AWG 36). The low thermal mass of these fine thermocouples allows them to react very quickly to changes in temperature. Each thermocouple was sampled at 1-s intervals (1 Hz) during the burn, and data were recorded on Campbell Scientific CR10 dataloggers. On plot 9, a taller tower (13.0 m) was deployed in the centre of the plot to measure temperatures higher into the tree canopy. This tower had thermocouples at heights of 1.5, 2.5, 3.5, 5.5, 7.5 9.0, 10.5, and 12.5 m; the uppermost thermocouple was near the top of the canopy. In the first 2 years of this study (1997–1998), shorter thermocouple towers (3.0 m in height) were also used in plots A, 5, 6, 7, and 8. They had the same type of thermocouple and sampling rate as the taller towers, but the thermocouples were fixed at 0.5, 1.0, 1.5, 2.0, 2.5, and 3.0 m. The number of thermocouple towers used per plot is summarized in Table 1.

Laboratory calibration and data analysis

The FTS thermologgers were tested for their ability to measure both flame arrival and flame residence in laboratory fires alongside a sensitive, fine-gauge, very low thermal mass thermocouple sampling at 1-s intervals. The FTS thermologger tracked the sensitive system quite well, with a lag time of about 10 s. This is probably due in part to the greater thermal mass of the FTS thermocouples. The time–temperature traces suggested that 500 and 300 °C were reasonable temperature thresholds to represent the occurrence of flaming combustion for the FTS thermologgers and fine-gauge thermocouples, respectively. Andersen (1970) found that the average surface temperature for ignition of forest fuels was 346 °C in the laboratory.

The paired time–temperature traces and visual observations afforded by the in-fire video footage suggested that for the FTS thermologgers, the >500 °C temperature threshold was correlated with the duration of flaming at the surface but that this overestimated the main flame front residence time because of residual flaming at the surface.

Analysis of variance was carried out to test for effects of plot and height above surface and on the maximum temperature and residence time using general linear model procedures (PROC GLM) in the SAS statistical facility. Effects were accepted as significant when the two-tail p value was <0.05.

Fig. 1. (A) 5-s average open wind speeds at 10-m height before, during, and after the burning periods (burning period in gray) at the control tower. (B) Spectral density of 5-s wind speed.

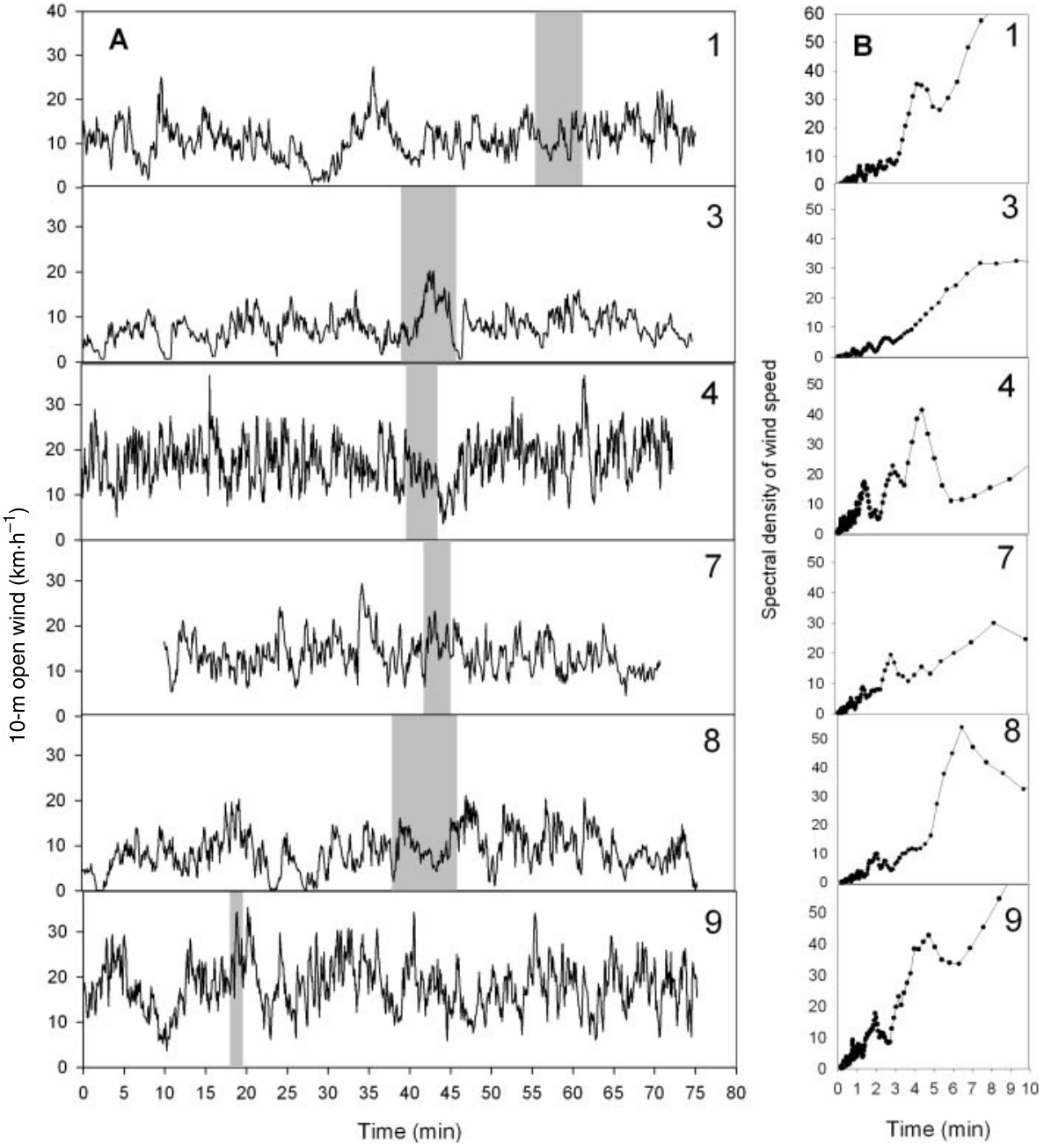

Results and discussion

Each plot was ignited along the edge that was exposed to and more or less perpendicular to the wind direction when the 10-m open wind speed was generally greater than 10 km·h^{-1}. In all plots except 2 (not reported on here), the fire spread from the surface to the crowns within 10 s of ignition and about 5 m from the plot edge, then spread through the plot and reached the opposite side. The fires crossed the plots in approximately 1.5–10 min, depending on the spread rate and plot size. This provided an opportunity to observe short-term and short-range variation in crown fire behaviour.

Wind-speed variation

Control tower 10-m open wind-speed traces for approximately 1 h before, during, and after each burning period (Fig. 1A) show a typical pattern of gusts and lulls. Autocorrelation analysis of these data suggests that the 5-s winds were stable for periods from about 45 s (plot 7) to 125 s (plot 8) during the burning periods. Spectral analysis of the raw wind data in the hour before and after the burning period suggests that there were periodicities in gust and lull peaks in the order of 130–180 s and 4–15 min (Fig. 1B).

Analysis of variance of the time course of 5-s wind speeds over the burning period at the control tower was carried out

Table 2. Wind speed, predicted rate of spread, and observed rate of spread (5-s averages).

		10-m control tower open wind speed					Predicted rate of spread[a]			Observed rate of spread		
Plot	n	Mean±SE ($km \cdot h^{-1}$)[b]	Max. ($km \cdot h^{-1}$)	Gust factor	Stable period (s)	Gust, lull frequency (s)	Mean±SE ($m \cdot min^{-1}$)	Max. ($m \cdot min^{-1}$)	Mean/max.	Mean±SE ($m \cdot min^{-1}$)	Max. ($m \cdot min^{-1}$)	Mean /max.
1	68	10.9±0.4a	17.5	1.60	120	250, 900	30.0±1.5	59.4	2.0	32.0±0.9	55.0	1.7
3	82	10.8±0.5a	20.3	1.87	100	155, 540	30.5±2.1	73.0	2.4	24.1±0.9	43.6	1.8
4	48	15.0±0.4b	20.8	1.38	70	180, 270	46.4±1.9	74.6	1.6	42.2±2.5	91.4	2.2
7	33	16.3±0.7b	23.4	1.44	45	170, 480	54.2±3.1	91.8	1.7	61.5±2.5	86.0	1.4
8	115	9.5±0.3a	16.2	1.71	125	110, 390	23.7±1.2	53.2	2.3	17.8±1.1	51.4	2.9
9	21	24.4±1.1c	34.4	1.41	105	110, 290	98.2±6.7	162.9	1.7	66.6±3.5	104.4	1.6

[a]Nelson and Adkins' (1988) model.
[b]Means followed by the same letter are not significantly different between plots.

for plots 1, 3, 4, 7, 8, and 9. The ANOVA suggests that there was a significant difference in mean wind speed between plots (burn days), but multiple comparison tests suggest that the mean wind speeds among plots 1, 3, and 8 and among plots 4 and 7 were not significantly different (Table 2). The average gust ratio (maximum/average wind speed) during the burning period over all plots was 1.6.

Time courses of wind speed at 5-s intervals during the burning period at the control tower and at the ignition face were not synchronous. The control tower and plot measures were taken at distances 100–700 m apart. Wind speeds were likely somewhat lower at the ignition face than in the open control because of differences in fetch, and the wind measures adjacent to the plots were also influenced by fire-induced circulation. Sullivan and Knight (2001) examined problems in measuring wind speed in experimental fires and found that the error in the mean wind speed taken at a point upwind may be as much as 30% different relative to a point 100 m downwind over a period of several minutes in a jarrah (*Eucalyptus marginata*) forest and that the error increases as the sampling time decreases.

In most of the fires, the wind direction was not exactly perpendicular to the ignition line or changed direction during the burning period; however, the major shifts in wind direction observed appeared to be associated with lulls (i.e., low wind speeds).

Effect of crown consumption on in-stand wind speed

The ratios of in-stand wind to control tower wind for each height both before and after burning are shown for plots 1 and 3 in Table 3. Ratios of in-stand wind to the plot edge winds measured at the tower in the fireguard between plots 1 and 3 are also presented. In the unburned stands, the ratio of in-stand/open winds increases with height above surface (i.e., decreases with distance from the top of the canopy). There is a marked increase in this ratio after the fire, and the differences with height are less pronounced. The ratios appear to be linear over a range of mean wind speeds in plot 1 (Fig. 2B). The change in ratios with height above ground surface is shown in Fig. 2C in relation to the vertical distribution of crown biomass (Fig. 2C) given in Alexander et al. (2004). Most of the foliage and fine branches were consumed during these fires, so that the residual stand consisted of tree boles and medium and large branches down to about 1.0 cm in diameter (Stocks et al. 2004*b*). The increase in the in-stand/open wind ratio suggests that as a crown fire is burning into a stand from an exposed edge, the drag exerted by the canopy is reduced as the crown fuels are consumed, and the fire has greater access to the ambient wind field over the whole flame length. This defoliation effect is analogous to wind patterns in deciduous forests. Quintilio et al. (1991) reported similar differences in the ratio of in-stand/open wind between leafed and leafless aspen stands. Allen (1968) found that there was greater eddy penetration in larch stands after needle drop in the fall, while Moore et al. (1996) found that the displacement height was lower in a leafless aspen stand than during leaf-out. We did not compare short-term variation in wind speed within the stands to assess the effect of jack pine canopy on gustiness and do not have enough wind measures with height to determine the inflection point in the canopy. However, it is likely that as the canopy foliage

Table 3. Comparison of preburn and postburn in-stand/open wind ratios.

Plot	Height (m)	Timing	In-stand/open wind ratio[a]	In-stand/plot edge wind ratio[a]
1	10	Preburn	0.253±0.005 (102)	0.342±0.007 (102)
1	10	Postburn	0.646±0.009 (202)	0.820±0.010 (197)
1	5	Preburn	0.136±0.005 (81)	0.232±0.006 (81)
1	5	Postburn	0.530±0.010 (168)	0.970±0.050 (163)
1	2	Preburn	0.135±0.002 (101)	0.221±0.005 (101)
1	2	Postburn	0.439±0.009 (202)	0.710±0.020 (197)
3	10	Preburn	0.186±0.003 (136)	0.241±0.004 (131)
3	10	Postburn	0.460±0.010 (66)	—
3	5	Preburn	0.071±0.003 (20)	0.120±0.010 (20)
3	5	Postburn	0.290±0.010 (40)	—
3	2	Preburn	0.198±0.005 (123)	0.321±0.009 (129)
3	2	Postburn	0.350±0.010 (66)	—

[a]Mean±SE (*n*).

Fig. 2. (A) Distribution of crown bulk density with height above ground in plot 1 (from Alexander et al. 2004, reproduced with permission of the Canadian Forest Service, © 2004 Her Majesty the Queen in right of Canada). (B) Relationship among 15-min average wind speeds at 2, 5, and 10 m above ground surface within plot 1 versus 10 m above open ground before (●) and after (○) burning. (C) Ratio of 15-min average 10-m open/in-stand wind speeds in plot 1 before (●) and after burning (○) in relation to canopy height.

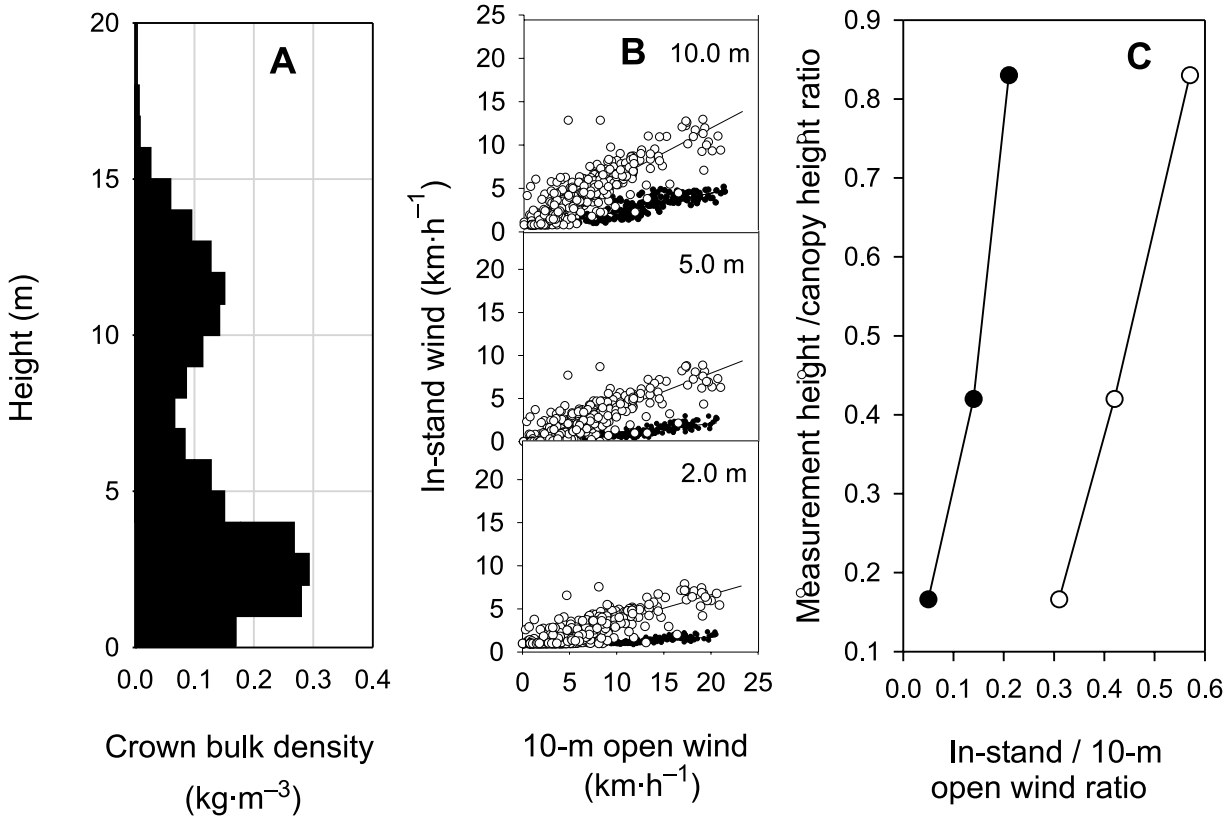

and fine branches are consumed by the crown fire, gustiness would increase along with mean wind speed, as downdrafts can better penetrate the residual canopy, and that the inflection point will be closer to the surface.

Flame front progression

As the flame front passed the thermocouples, the fire-arrival times and temperatures were recorded at the surface, and a number of observations of fire progression within the stand were recorded on videotape. A total of 18 video clips were inspected from within nine active crown fires in 1998, 1999, and 2000. Eight of these were from five fires in the main plots (1, 3, 4, 8, 9), while the others were in plots not reported here. A sequence of still photos extracted from videotape taken in plot 3 are shown in Fig. 3. The fire approached from behind the camera at a spread rate of about 20–30 m·min^{-1} (i.e., ~0.30–0.5 m·s^{-1}). The sequence shows glowing and flaming embers starting numerous spot fires approximately 10–20 m ahead of the flame front (Fig. 3A); gasses coming off tree boles about 7 m ahead of the flame

Fig 3. Crown fire progression beneath the canopy in plot 3 recorded over 2.5 min on June 28, 2000. The rate of spread is about 20–30 m·min^{-1} (0.35–0.5 m·s^{-1}). (A) 15:08:26, spot fire starts from ember rain about 10 m ahead of the flame front. (B) 15:08:40, vapor release from bark on tree boles at about 6 m ahead of the flame front. (C) 15:08:48, ignition of forest floor patches and tree boles about 3–4 m ahead of the flame front. (D) 15:08:52, arrival of continuous flame front. (E) 15:09:02, flaming below canopy. (F) 15:10:57, residual flaming of forest floor, downed woody debris, and tree boles.

Fig. 4. Kriged fire spread isochrons and rate of spread surfaces for nine experimental crown fires. For comparison purposes, the plots were rotated such that ignition is in on the left and fires are spreading to the right in each case; plot numbers are under each map.

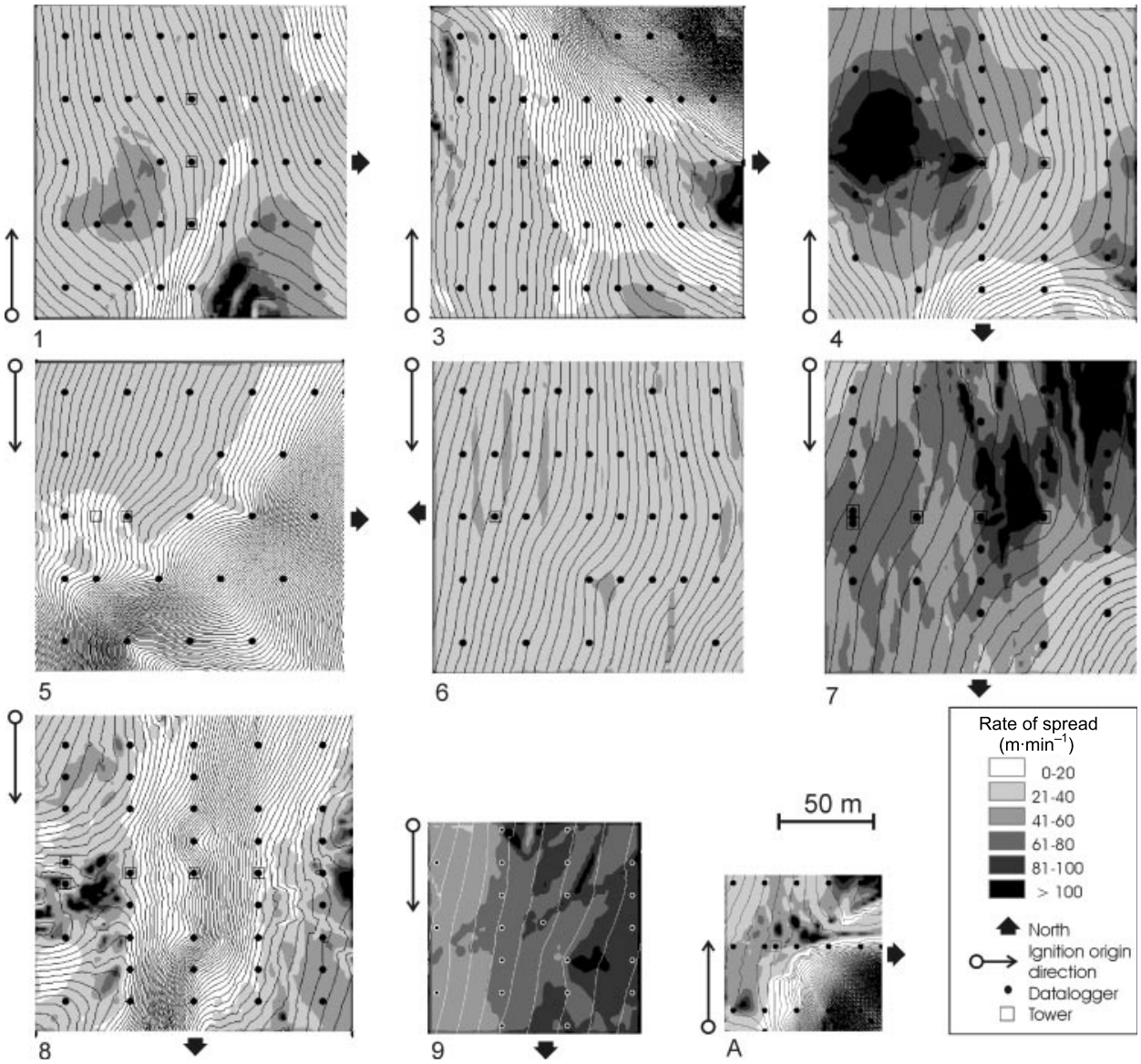

front, presumably because of radiant heating (Fig. 3B); and an ignition zone ahead of the fire, where small patches of forest floor material, especially terrestrial lichens, and bark flakes on tree boles about 3–5 m above ground level are igniting before the main flame front or perhaps as the flame front fills in and the spot fires coalesce (Fig. 3C).

The spotting is likely a result of updrafts produced by convective activity. Based on analysis of high-speed, infrared video taken at ground level along the side of plot 6, Clark et al. (1999) estimated updraft wind speeds of 10–30 m·s^{-1}, downdraft speeds of 10–30 m·s^{-1}, and horizontal wind speeds of 5–15 m·s^{-1} around the flame front, although the latter are in the order of metres in scale.

One consequence of this piloted ignition mechanism ahead of the main fire front is that the ignition temperature is lower for piloted ignitions than for spontaneous ignition from radiant heating alone (Beer 1991). Fons (1946) noted that rate of fire spread may be visualized as proceeding by a series of successive ignitions, its magnitude controlled primarily by the ignition time of the particles and the distance between them. These photographs illustrate that fuel elements ahead of the flame front ignite at different times, and so the flame front at the surface and below the canopy is not continuous at the scale of the fuel element. Ignition time likely depends on the exposure to radiation, surface area/volume ratio, and moisture content of the fuel elements. The rate of fire spread (m·s^{-1}) is thus the remainder of the ignition zone depth (m) divided by the ignition time (s) of the fuel particles within it.

Kriging techniques were used to model fire spread from a grid of fire-arrival times for each fire. Contours of the resulting time surfaces (isochrons) are a smoothed representation of the flame location over time (Fig. 4). The fit of the fire-arrival time surfaces was generally good (Table 4). The variation in fit is probably due to the number of sample points included and the complexity of the spread pattern. The poor-

Table 4. Summary of cross-validation statistics for the kriged fire-arrival time surfaces.

	Plot								
Parameter	1	3	4	5	6	7	8	9	A
Mean error	–0.50	–2.50	2.34	6.46	–0.38	1.38	0.45	0.33	–22.88
Root mean square error	13.91	137.4	22.05	74.13	20.53	8.96	59.9	10.6	285.4
Average standard error	5.68	55.17	7.71	13.74	14.79	3.74	25	7.27	32.06
Mean standardized error	–0.08	–0.02	0.30	0.47	–0.02	0.33	0.02	0.04	–0.69
Root mean square standardized error	2.45	2.33	2.86	5.34	1.38	2.32	2.40	1.46	8.72
R^2	0.97	0.69	0.88	0.86	0.94	0.96	0.91	0.87	0.34

est overall time surface fits were in plots 3 and A (r^2 = 0.69 and 0.34, respectively), where the head fire spread diagonally through the plot, then the flank continued to spread at a slower rate. A better fit of the time surfaces for these fires might have been achieved by fitting separate surfaces for regions with distinct spread rates.

Rates of spread were calculated from the slope of the fire-arrival surface. The rate of spread class maps shown in Fig. 4 suggest that with the exception of plot 6, fire spread rate was highly variable in both time and space for experimental fires of this scale (fires spreading over 75–150 m for 1.5–10 min). The fires spread at a rapid rate immediately following ignition with no apparent acceleration and did not develop a distinctive head, perhaps because of the relatively small plot size relative to the scale of the process. Cheney and Gould (1995) found that experimental grass fires developed a distinctly parabolic head shape that they proposed was caused by downdrafts causing advective heating. Downdrafts may have less influence in crown fires because of the presence of the forest canopy and stronger updrafts above the flame zone (Clark et al. 1999).

Certain areas within plots 1, 3, 7, and 9 experienced quite high spread rates of the order of 40–60 s duration, with a width of about 30–50 m perpendicular to the spread direction. In plots 3, 5, and 8, there were periods where spread rates dropped appreciably for a period of 100 s to several minutes. Drops in rate of spread appeared to be related to lulls in wind speed, especially in plot 8, where rate of spread dropped dramatically for about 5 min during the burning period when the wind speed dropped below 10 km·h^{-1}. This may be because the wind speed and associated fire spread and intensity were below the critical threshold for crowning as set out in Van Wagner's (1977) theory regarding crown fire initiation. The difference between wind speed in the open and that within a burned stand suggests that if a fire drops from the crown to the surface, a greater wind speed may be needed to reinitiate crowning than to initiate it in an opening or at the stand edge.

Van Wagner (1977) noted that evidence of the interaction of short-term variation in wind speed with stand structure and topography can often be seen in aerial photos of large burned areas, and he presented a predictive equation for crown fraction burned as a function of the surface fire spread rate and the critical fire spread rate for crowning (Van Wagner 1993). However, a physical mechanism to explain intermittent crowning has not been proposed. The occurrence of intermittent crowning may be due to short-term variation in wind speed as well as variation in crown fuel properties. If this is the case, crown fraction burned might be modeled stochastically from the variance in wind speed.

The location of the point of maximum rate of spread at 1-s intervals was estimated from the rate of spread and time surfaces, excluding a 10-m buffer at the plot edges, and is shown in Fig. 5. The track of the points from left to right indicates the spread direction. In plots 1, 3, 4, and 8, there appear to be regions where the head fire follows distinctly different tracks, suggesting that the point of maximum spread shifts across the fire front in a discontinuous manner over time. This may be due to wind-speed turbulence and the structure of gusts. That is, as the fire progresses and the wind speed rises and falls, wind speed may increase to a greater degree at some point along the fire front other than at the head, and that fire may accelerate at that point and form a new head.

Short-term and short-range variations in fire spread may not be significant in predicting fire spread distance over several hours for the purpose of planning control efforts or evacuations. However, short-term variation in spread rate will be reflected in variation in fire intensity following Byram's (1959) equation: $I = Hwr$ where I, H, w, and r are fire intensity (kW·m^{-1}), heat of combustion (kJ·kg^{-1}), fuel consumption (kg·m^{-2}), and rate of spread (m·s^{-1}), respectively. Fine-scale variation in fire intensity may be important in understanding processes that are dependent on the distribution of fire intensities rather than on the mean fire intensity (Alexander 1982). These processes may include prediction of intermittent crowning, including the implications to ecological effects such as crown scorch height and tree mortality, and the probability of fireguard breaching. For example, de Groot et al. (2004) found significant spatial variation in viable seed rain following burning of these plots, which was not well explained by the mean fire intensity but may be due to within-plot variation in fire intensity.

Wind speed and rate of spread correlation

To examine the relationship between fire spread and wind speed, we estimated the position of the point of maximum spread rate at 1-s intervals and the average maximum fire spread rate over 5-s intervals from the fire-arrival time and rate of spread surfaces (Table 2). The maximum fire spread rates were averaged over 5 s to be consistent with the wind-speed measurements; 5 s is longer than the mean error and root mean square standardized error of the arrival time surfaces in most of the plots (Table 4). The average gust factor (maximum/average wind speed) was 1.6, while the average maximum/average rate of spread rate was 1.9. This suggests that there is greater short-term variance in rate of spread than in wind speed.

The 5-s measures of control tower and plot edge wind speed were significantly but inconsistently correlated with

Fig. 5. Estimated position of the point of maximum rate of spread at 1-s intervals for nine experimental crown fires. For comparison purposes, the plots were rotated such that ignition is on the left and fires are spreading to the right in each case; plot numbers are under each map.

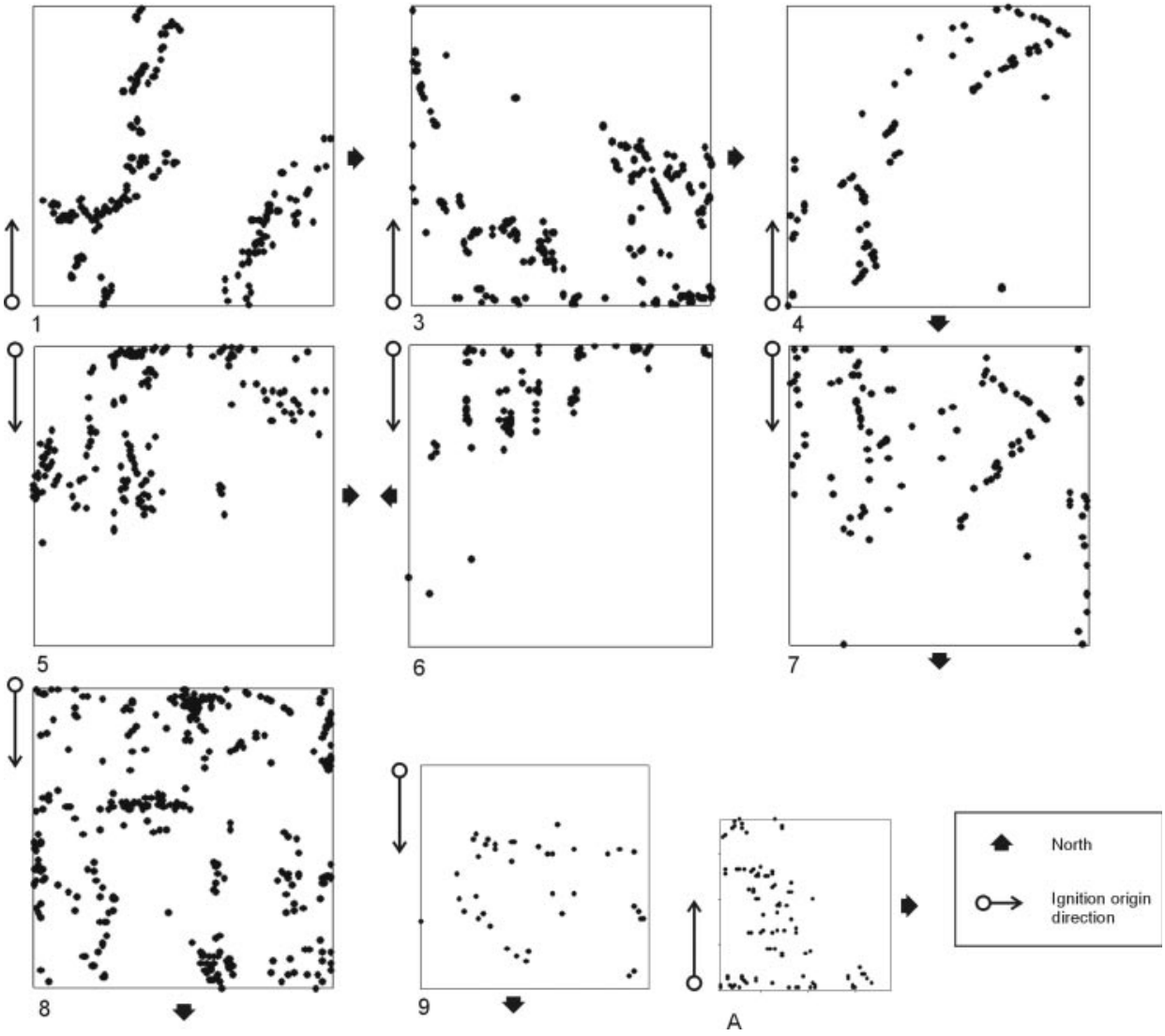

Table 5. Simple correlation coefficients (r) between 5-s average wind speed and rate of spread.

	Plot					
Parameter	1	3	4	7	8	9
Rate of spread vs. 10-m control tower wind	–0.18	–0.55**	0.46**	0.31**	0.40**	0.27
Rate of spread vs. 10-m plot edge wind	0.25*	–0.31**	0.01	0.05	0.14	0.50*

rate of spread (Table 5). Cheney et al. (1993) also found that short-term spread rates and wind speed were poorly correlated. This may be due in part to the lag between the measurement of wind at the ignition edge and the wind acting at the flame front. Wind gusts of 20–40 km·h^{-1} (approximately 5–10 m·s^{-1}) measured 10 m from the ignition edge would take approximately 16–32 s to reach the end of the 150-m plot. We did not attempt to correct for the lag in relation to the movement of the fire front in this study. Sullivan and Knight (2001) found that using Taylor's frozen eddy hypothesis (Kaimal and Finnigan 1994) to correct for lag is not appropriate within forest stands, possibly because of within-canopy turbulence.

Attempts to correlate wind speed and rate of spread are confounded by difficulties in measuring temporal and spatial variation in both wind speed and rate at compatible scales. We can measure wind speed at intervals in the order of 1–10 s and the vertical variation in wind speed at one or several points in space, but we cannot easily measure the horizontal variation or measure the wind acting on the moving flame zone, which is further confounded by fire-induced circulation. In contrast, we can estimate fire spread rates over dis-

Table 6. Mean maximum temperatures (°C) by height above surface.

	Height (m)[a]			
Plot	0.01–1.5	2.0–4.0	4.01–7.0	>7.01
1	1150±21 (4)	1152±91 (6)	1060±70 (4)	1051 (1)
3	1041±23 (5)	1053±15 (5)	765±58 (6)	809±76 (3)
4	986±162 (6)	1068±37 (6)	1056±40 (4)	1046±166 (3)
5	1155±7 (2)	1008±2 (3)	945 (1)	905 (1)
6	1144±24 (2)	1178±24 (3)	—	1159±(1)
7	1172±34 (4)	1206±3 (4)	1125±113 (4)	1200±42 (2)
8	1069±34 (4)	1013±58 (4)	1072±84 (4)	1090±42 (2)
9	1105±31 (5)	1104±40 (5)	1180±15 (4)	1294±118 (6)
A	1195±48 (2)	1216 (1)	—	1239 (1)

[a]Mean±SE (*n*).

Fig. 6. Typical time–temperature traces with height above ground surface just prior to, during, and immediately following flame front passage at plot 3 for the thermocouple array depicted in Fig. 1.

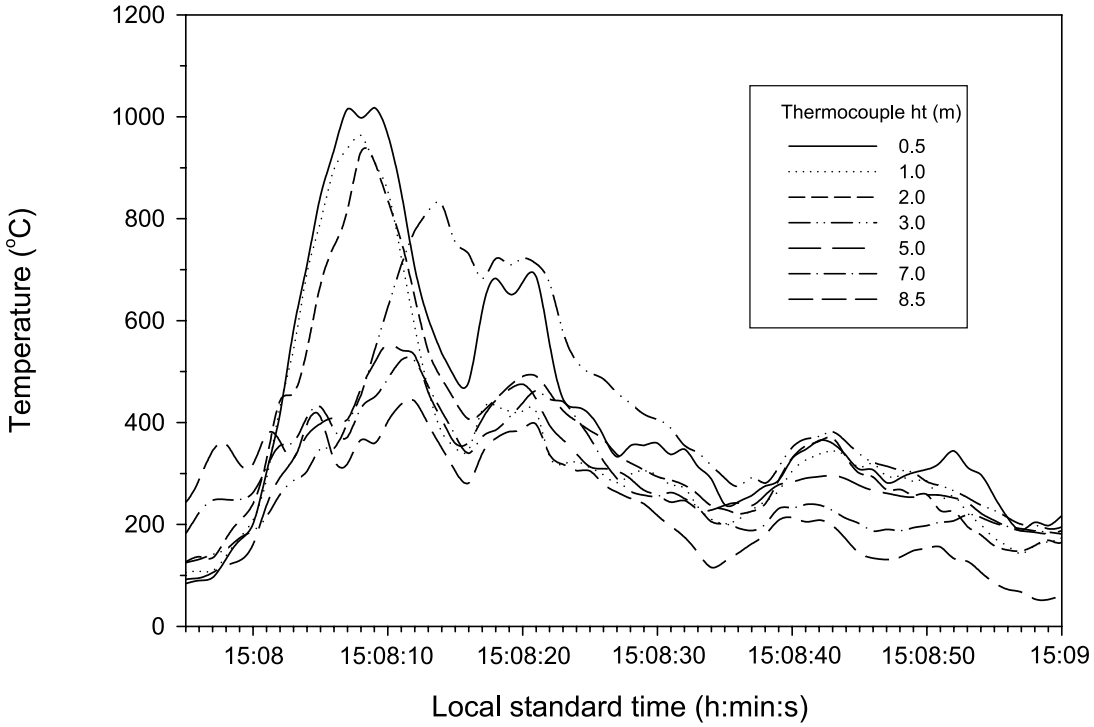

tances of tens of metres, but for fast-moving fires we were not able to resolve the temporal variation below about 10 s.

Flame temperature and flaming front residence time

As the main flame front spread through the plots, the in-fire camera boxes were bathed in flame (Figs. 3D and 3E). Three independent observers reviewed in-stand video of the fire progression and made visual estimates of the duration of flaming below the canopy. The estimates of flame front arrival to end duration ranged from 29 to 37 s (with a mean of 34 s) for the four fires presented in Table 6 and were consistent with estimates from the five other fires, which are not reported here. There was less variation in the estimates of fire arrival than in the estimates of the end of flaming because of residual flaming at the surface and of tree boles (Fig. 3F). Following the passage of the flame front, flaming of the forest floor, downed debris, and tree boles continued for approximately 1 min on average, with a range of 30–150 s.

The measurement of air and flame temperatures in a fire is complicated by influences of radiation (Jones 1993). The temperature of a thermocouple depends on the net energy received, and thus it may not be the same as the air or flame temperature. The use of small-diameter thermocouples, with very small thermal mass and cross section, can limit the error due to radiative heating and cooling (see Butler et al. 2004 for a more detailed description). Laboratory studies have revealed that the temperature of the visible flame tip from burning forest fuels is consistently around 300 °C over a range of heights. Time–temperature traces from each of the primary plots were examined during the passage of the flame front to estimate variation in flaming duration at the forest floor surface and above the forest floor. Traces from

Table 7. Estimates of flame front residence times (s) from video observations and interpretation of time–temperature traces.

			Time vertical temperatures above 300 °C by height (m)[a]			
Plot	Video estimates at 1.3 m	Time surface temperatures >500 °C[a]	0.01–1.5	2.0–4.0	4.01–7.0	>7.01
1	29 (3)	63±5 (44)	34±5 (4)	26±3 (6)	21±2 (4)	28 (1)
3	35 (4)	85±5 (41)	44±4 (5)	29±4 (5)	21±2 (6)	19±1 (3)
4	—	80±7 (41)	32±7 (6)	23±2 (6)	24±6 (4)	28±8(3)
5	—	94±13 (23)	50±8 (2)	22±2 (3)	33 (1)	30 (1)
6	—	71±11 (23)	45±10 (2)	33±2 (3)	—	24 (1)
7	—	67±5 (24)	118±45 (2)	81±32 (2)	64±28 (2)	36 (1)
8	37 (1)	69±6 (24)	93±13 (2)	70±4 (2)	—	—
9	34 (1)	70±7 (22)	43±4 (4)	41±5 (5)	43±4 (4)	42±4 (5)
A	—	65±8 (15)	61±0 (2)	54 (1)	—	45 (1)
Mean	34	74	58	42	34	31

[a]Mean±SE (*n*).

thermocouples that broke during the fire or provided a suspect signal were excluded from the analysis. Suspect signals were defined as those exhibiting a rise and fall in temperature dissimilar from that of other thermocouples at the same point, most likely because of degradation of insulation and shorting of the thermocouple leads.

A representative time–temperature trace (Fig. 6) shows a very rapid rise in temperature from ambient levels as the flame arrives. While there is considerable fluctuation in temperature when the thermocouple is within the flaming zone, temperature generally fluctuates around some sustained maximum value and then drops down rapidly as the main area of flaming passes the thermocouple. This is a typical pattern for wildland fires (Weber et al. 1995; Ryan 2002). In general, the temperature then remains above ambient for 1–2 min, slowly cooling as the heat from the forest floor slowly dissipates. The low thermal mass (and rapid response time) of the fine thermocouples used on the temperature towers means stored temperature is not causing false, sustained high temperatures and are revealing a fairly accurate estimate of the actual air temperature during this portion of the fire.

All of the fires were actively spreading crown fires, with flames well above the canopy and with broadly similar flame structure. For the vertical temperature arrays, the length of time that temperature measured at a point was above threshold temperatures of 300 °C was examined for each thermocouple trace. Maximum temperatures (recorded at 1-s intervals) at each point were also studied. Temperature measured at a single point in a fire can vary rapidly with time and be different over short distances because of differences in the structure of the vertical fuel available to the fire. Owing to logistical constraints and equipment failures, we were often not able to obtain replicated observations of temperature at each height within each plot. Thus, we decided it was most representative to examine average values by height class for each of the plots. The thermocouple heights were grouped into four height classes: 0.01–1.5; 2.0–4.0; 4.01–7.0; and >7.01 m.

Analysis of variance was carried out on maximum temperatures measured within each of these height classes to determine if there was a real height effect that the grouping might have obscured. Within each height class grouping, no significant influence of the actual height of the thermocouple on maximum temperature measured was observed (Table 6). A further analysis of variance examining the influence of height class and plot on maximum temperature showed there was a significant plot-to-plot effect but no significant difference in maximum temperature with height across the full range of heights measured in this experiment. This should not be interpreted to mean there is no difference in maximum flame temperature with height below and within the canopy in actively spreading crown fires, but that given the large observed variance in this element, the number of replicates at each level (which varied from 1 to 6) did not reveal a difference. Indeed, Butler et al. (2004) observe such a trend in maximum temperature with height; however, they did not report conclusively on its statistical significance. The highest mean maximum temperature measured (1294 °C) was at the highest level above ground (12.5 m) on plot 9 (Table 5). The within-plot variability observed in maximum temperature suggests that greater replication of these vertically stratified flame temperature measurements is needed to make any conclusive inferences about the vertical structure of flames within the canopy space of crown fires. The within-plot variability in temperature measures is also consistent with fine-scale variability in fire intensity.

A similar analysis of variance was carried out on the duration above the 300 °C threshold. First, an analysis of variance was used within height class to examine for an influence of actual height on duration above the 300 °C threshold; no such influence was observed. A further analysis of variance examining the influence of height class and plot on time above 300 °C showed there was a significant plot effect and also a significant difference with height. The duration of exposure to temperatures above 300 °C generally decreased with height (Table 7), which suggests that the estimates of front flame residence time below the canopy from video recording overestimate the residence time in the crown layer. The canopy flame front residence times observed in this study were somewhat greater than the average of 15–20 s reported by Despain et al. (1996) from video analysis of crown fires in lodgepole pine during the 1988 Yellowstone fires. An-

Fig. 7. (A) Frequency distribution of 5-s average wind speeds at 10 m for approximately 60 min around the burning period (heavy line) and during the burning period (shaded grey). (B) Frequency distribution of predicted 5-s average rate of spread from Nelson and Adkins' (1988) model for approximately 60 min around the burning period (heavy line) and during the burning period (shaded grey). (C) Frequency distribution of observed 5-s average maximum rate of spread values during the burning period. Plot numbers are on the upper right of each frame.

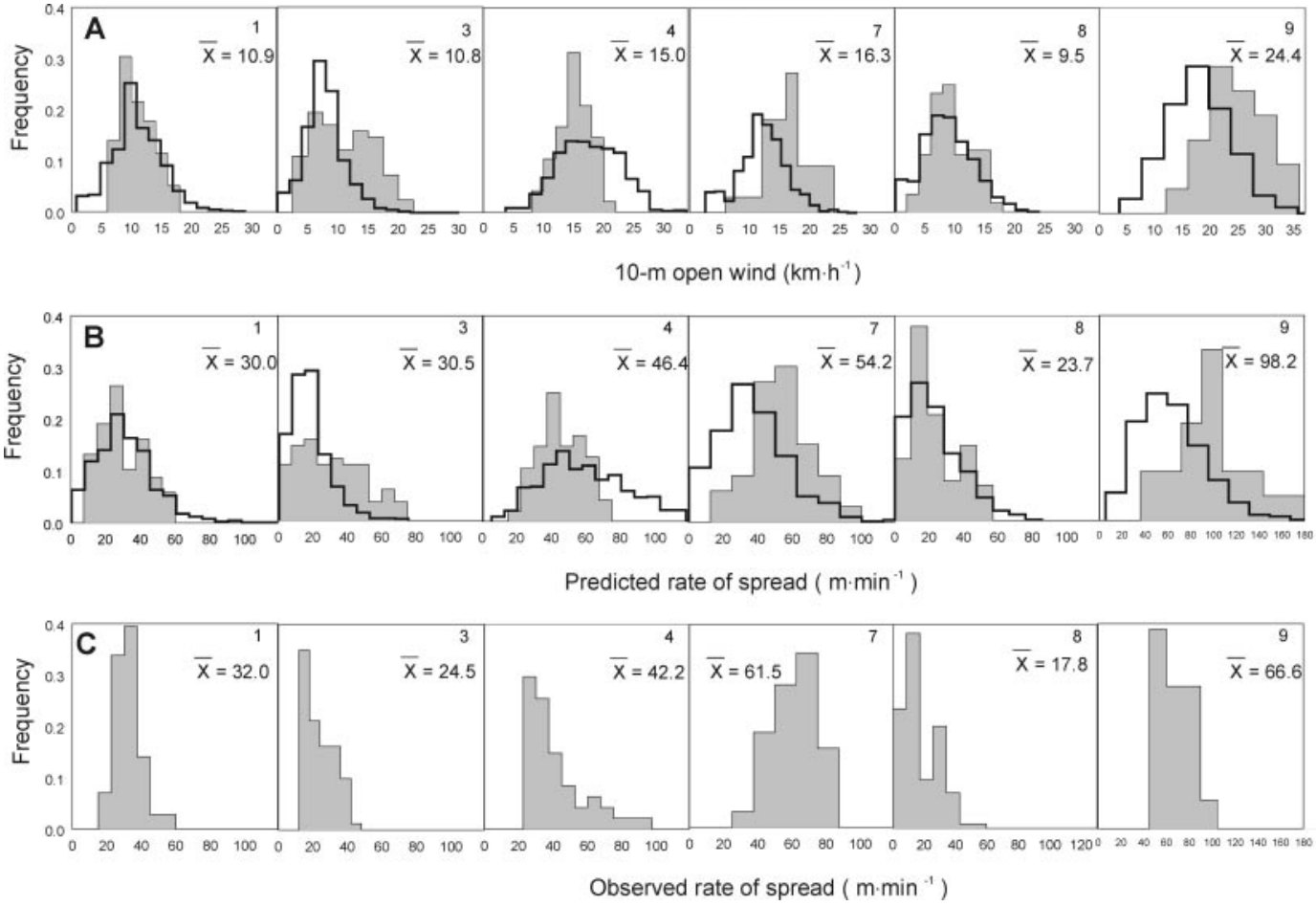

derson (1969) found that the flame residence time of forest fuels in the laboratory was related to particle size and packing ratio. From his model, fine branches 0.5 mm in diameter would have a residence time in the order of 20–30 s. Burrows (2001) also found a similar relationship between fuel particle diameter and residence time in the laboratory.

Modeling effects of variation in wind speed on rate of spread

Stocks et al. (2004*b*) found that Nelson and Adkins' (1988) model (eq. 1) predicted the mean spread rates for the main plots in this experiment fairly well using mean wind-speed measures at the control tower over the burning period and residence times of 30 and 45 s. The fastest-spreading fire (plot 9) had the poorest fit. This may be because the average wind speed was determined from observations at the control tower over a short (100 s) burning period, and the difference in average measures of wind at different locations will increase as the measurement period decreases (Cheney et al. 1993; Sullivan and Knight 2001).

We applied Nelson and Adkins' (1988) model to examine the effect of variation in wind speed on rate of spread predictions using 5-s average 10-m open wind speeds (Fig. 1), mean plot fuel consumption, and residence times of 20 s as input variables. However, because Nelson and Adkins' (1988) model is based on a mid-flame wind speed, we applied the postburn in-stand/open 10 m wind ratio of 0.6 from plot 1 (Table 3 and Fig. 2C) to reduce the wind velocity at the rear of the fire from open wind-speed measures.

Frequency distributions of 5-s average wind speed and predicted rates of spread for each burning period at about 1 h around the burning period are shown in Fig. 7 along with distributions of observed rates of spread. The means of rate of spread values calculated from 5-s wind-speed measures are somewhat larger than the mean rates of spread calculated from the mean wind speed (Stocks et al. 2004). This bias was because rate of spread is proportional to wind speed to the 1.51 power in Nelson and Adkins' (1988) model.

More importantly, the ranges of predicted and observed rates of spread for the burning period (grey shaded portion of Figs. 7B and 7C) are similar. The observed rates of spread (for periods of 1.5–10 min) also encompass a surprisingly large portion of the predicted variation in rate of spread for the 1-h periods (heavy line in Fig. 7B). This suggests that the magnitude of variation in rate of spread over burning periods of an hour or so can be estimated from short-term mea-

sures of wind variance using the Nelson and Adkins' (1988) and perhaps other empirical models, such as the Canadian FBP System.

Wind-speed distributions are often modeled using a Weibull function. If fire spread rate is a power function of wind speed (as in the Nelson and Adkins' (1988) model), then fire spread rates should have a gamma-like distribution, i.e., the right tail of the distribution representing higher spread rates should be amplified. This is suggested by the distributions of predicted rate of spread for the 1-h periods (heavy line in Fig. 7B) and to a lesser extent in the distributions of observed rate of spread (Fig. 7C). The observed rate of spread distributions are based on a relatively small number of estimates because of the short burning periods (e.g., only 90 s for plot 9), and they may have been truncated at the tails because of the density of the sample points and surface smoothing.

Conclusions

Most empirical fire spread models assume a quasi-steady state or equilibrium rate of spread (Cheney 1981). However, rate of spread estimates during crown fires show considerable variation within distances of up to 150 m over periods of 1.5–10 min. The short-term and short-range variation in rate of spread and intensity may be in the same order of magnitude as the variation that would be expected over burning periods of an hour and thousands of metres.

Variance in fire spread appears to be greater than variance in wind speeds, and higher values are amplified. Greater variation in fire spread rate may also be because of variation in fuel characteristics and moisture content across the plots.

Cheney (1981) notes that some of the mystery associated with fire behaviour and the consequent fire effects has resulted from inadequate descriptions of fire types and inadequate measurements of important flame characteristics and fire behaviour phenomena. Inadequate description of the variability of fire phenomena may also be a factor.

In operational fire management, the prediction of average spread rate is important to plan the placement of suppression lines or evaluate the threat to structures or other values at risk. However, estimation of the fire spread rate and intensity distribution may be important in assessing fire fighter safety, effectiveness of constructed fire lines and retardant drops, and ecological effects. Explicitly incorporating estimates of short-term variation in wind speed characteristic of different atmospheric stability conditions in crown fire models may improve predictions of spread rate, the probability of crowning, variation in fire intensity associated with the head fire, and in turn the ecological effects.

Acknowledgements

Appreciation is extended to the following individuals who assisted with the field work associated with this paper: J. Mason, G. Hartley, T. Blake, C. Stefner, B. Hawkes, B. de Groot, K. Hirsch, V. Kafka, B. Todd, J. Trentmann, and T. Zorn. Thanks also go to R. Coombs for constructing the insulated camera box, J. Kautz for loan of additional video equipment and insulated boxes, S. Glover for editorial assistance, G. Thandi for assistance with GIS procedures, and to J. Beck and three anonymous referees for reviewing an earlier draft of this paper.

References

Albini, F.A. 1982*a*. Response of free burning fires to nonsteady wind. Combustion Science and Technology, **29**: 225–241.

Albini, F.A. 1982*b*. The variability of wind-aided free burning fires. Combust. Sci. Technol. **31**: 303–311.

Alexander, M.E. 1982. Calculating and interpreting forest fire intensities. Can. J. Bot. **60**: 349–357.

Alexander, M.E., Stefner, C.N., Mason, J.A., Stocks, B.J., Hartley, G.R., Maffey, M.E. et al. 2004. Characterizing the jack pine – black spruce fuel complex of the International Crown Fire Modelling Experiment (ICFME). Can. For. Serv. Inf. Rep. NOR-X-393.

Allen, L.H. 1968. Turbulence and wind speed spectra within a Japanese larch plantation. J. Appl. Meteorol. **7**: 73–78.

Anderson, H.E. 1969. Heat transfer and fire spread. USDA For. Serv. Res. Pap. INT-69.

Anderson, H.E. 1970. Forest fuel ignitability. Fire Technol. **6**: 312–319, 322.

Anderson, D.H., Catchpole, E.A., DeMestre, J.J., and Parkes, T. 1982. Modeling the spread of grass fires. J. Aust. Math. Soc. **23**: 451–466.

Beer, T. 1991. The interaction of wind and fire. Boundary-Layer Meteorol. **54**: 297–308.

Boettcher, F., Renner, C.H., Wadl, H.-P., and Peinke, J. 2003. On the statistics of wind gusts. Boundary-Layer Meteorol. **108**: 163–173.

Burrows, N.D. 2001. Flame residence times and rates of weight loss of eucalypt forest fuel particles. Int. J. Wildland Fire, **10**: 137–143.

Butler, B.W., Cohen, J., Latham, D.A., Schuette, R.S., Sopko, P., Shannon, K.A, Jimenez, D., and Bradshaw, L.R. 2004. Measurements of radiant emissive power and temperatures in crown fires. Can. J. For. Res. **34**. This issue.

Byram, G.M. 1959. Combustion of forest fuels. *In* Forest fire: control and use. *Edited by* K.P. Davis. McGraw-Hill, New York. pp. 61–89.

Cheney, N.P. 1981. Fire behavior. *In* Fires and the Australian biota. *Edited by* A.M. Gill, R.H. Groves, and I.R. Noble. Australian Academy of Sciences, Canberra. pp. 151–175.

Cheney, N.P., and Gould, J.S. 1995. Fire growth in grassland fuels. Int. J. Wildland Fire, **5**: 237–247.

Cheney, N.P., Gould, J.S., and Catchpole, W.R. 1993. The influence of fuel, weather, and fire spread variables on fire spread in grasslands. Int. J. Wildland Fire, **3**: 31–44.

Cheney, N.P., Gould, J.S., and McCaw, L. 2001. The Dead-Man Zone: a neglected area of firefighter safety. Aust. For. **64**: 45–50.

Clark, T.L., Jenkins, M.A., Coen, J., and Packham, D. 1996. A coupled atmosphere–fire model: convective Froude number and dynamic fingering. Int. J. Wildland Fire, **6**: 177–190.

Clark, T.L., Radke, L., Coen, J., and Middleton, D. 1999. Analysis of small-scale dynamics in a crown fire using infrared video imagery. J. Appl. Meteorol. **38**: 1401–1420.

Crosby, J.S., and Chandler, C.C. 2004. Get the most from your wind speed observation. Fire Manage. Today, **64**: 53–55.

de Groot, W.J., Bothwell, P.M., Taylor, S.W., Wotton, B.M., Alexander, M.E., and Stocks, B.J. 2004. Jack pine regeneration and crown fires. Can. J. For. Res. **34**. This issue.

Despain, D.G., Clark, D.L., and Reardon, J.J. 1996. Simulation of crown fire effects on canopy seed bank in lodgepole pine. Int. J. Wildland Fire, **6**: 45–49.

Finnigan, J. 2000. Turbulence in plant canopies. Annu. Rev. Fluid Mech. **32**: 519–571

Finnigan, J.J., and Brunet, Y. 1995. Turbulent airflow in forests on flat and hilly terrain. *In*Wind and trees. *Edited by* M.P. Coutts and J. Grace. Cambridge University Press, Cambridge, UK. pp. 3–40.

Fons, W.L. 1946. Analysis of fire spread in light forest fuels. J. Agric. Res. **72**: 93–121.

Forestry Canada Fire Danger Group. 1992. Development and structure of the Canadian forest fire behavior prediction system. Can. For. Serv. Inf. Rep. ST-X-3.

Jones, J.C. 1993. Combustion science: principles and practice. Millennium Books, Sydney, New South Wales.

Johnston, K., Ver Hoef, J.M., Krivoruchko, K., and Lucas, N. 2001. Using ArcGIS Geostatistical Analyst. Environmental Systems Research Institute, Redlands, Calif.

Kaimal, J.C., and Finnigan, J.J. 1994. Atmospheric boundary layer flows: their structure and measurement. Oxford University Press, New York.

Kautz, J. 1997. Appendix C — insulated boxes for protecting video cameras. *In* Surviving fire entrapments: comparing conditions inside vehicles and fire shelters. *Edited by* R. Mangan. USDA For. Serv. Missoula Tech. Dev. Cent. Tech. Rep. 9751-2817-MTDC. pp. 39–40.

Linn, R.R, Reisner, J., Coman, J.J., and Winterkamp, J. 2002. Studying wildfire behavior using FIRETEC. Int. J. Wildland Fire, **11**: 233–246.

Moore, K.E., Fitzjarrald, D.R., and Sakai, R.K. 1996. Seasonal variation in radiative and turbulent exchange at a deciduous forest in central Massachusetts. J. Appl. Meteorol. **35**: 122–134.

Morvan, D., Tauleigne, V.,and Dupuy, J.L. 2002. Wind effects on wildfire propagation through a Mediterranean shrub. *In* Forest fire research and wildland fire safety. *Edited by* D.X. Viegas. Milpress, Rotterdam. pp. 1–13.

Nelson, R.M., and Adkins, C.W. 1988. A dimensionless correlation for the spread of wind-driven fires. Can. J. For. Res. **18**: 1–397.

Quintilio, D., Alexander, M.E., and Ponto, R.L. 1991. Spring fires in a semimature trembling aspen stand in central Alberta. Can. For. Serv. North. For. Res. Cent. Inf. Rep. NOR-X-323.

Raupach, M.R., Finnigan, J.J., and Brunet, Y. 1996. Coherent eddies and turbulence in vegetation canopies: the mixing layer analogy. Boundary-Layer Meteorol. **78**: 351–382.

Reifsnyder, W.E. 1955. Wind profiles in a small isolated forest stand. For. Sci. **1**: 289–297.

Rothermel, R.C. 1972. A mathematical model for predicting fire spread in wildland fuels. USDA For. Serv. Res. Pap. INT-115.

Ryan, K.C. 2002. Dynamic interactions between forest structure and fire behavior in boreal ecosystems. Silva Fenn. **36**: 13–39.

SAS Institute Inc. 1993. SAS/ETS user's guide, version 6. SAS Institute Inc., Cary, N.C.

Simard, A.J., Deacon, A.G., and Adams, K.B. 1982. Non-directional sampling of wildland fire spread. Fire Technol. **18**: 221–228.

Simard, A.J., Eenigenburg, J.E., Adams, K.B, Nissen, R.L., Jr., and Deacon, A.G. 1984. A general procedure for sampling and analyzing wildland fire spread. For. Sci. **30**: 51–64.

Sneeuwagjt, R.J., and Peet, G.B. 1985. Forest fire behavior tables for western Australia. Department of Conservation and Land Management, Western Australia.

Stocks, B.J., Alexander, M.E., and Lanoville, R.A. 2004*a*. Overview of the International Crown Fire Modelling Experiment (ICFME). Can. J. For. Res. **34**. This issue.

Stocks, B.J., Alexander, M.E., Wotton, B.M., Stefner, C.N., Flannigan, M.D., Taylor, S.W. et al. 2004*b*. Crown fire behaviour in a northern jack pine – black spruce forest. Can J. For. Res. **34**. This issue.

Sullivan, A.L., and Knight, I.K. 2001. Estimating error in wind speed measurements for experimental fires. Can. J. For. Res. **31**: 401–49.

Van Wagner, C.E. 1977. Conditions for the start and spread of crown fire. Can. J. For. Res. **7**: 23–34.

Van Wagner, C.E. 1987. Development and structure of the Canadian forest fire weather index system. Can. For. Serv. For. Tech. Rep. 35.

Van Wagner, C.E. 1993. Prediction of crown fire behavior in two stands of jack pine. Can. J. For. Res. **23**: 442–449.

Weber, R.O., Gill, A.M., Lyons, P.R.A., and Mercier, G.N. 1995. Time dependence of temperature above wildland fires. CALMScience Suppl. 4: 17–22.